THERMOELASTIC STABILITY ANALYSIS OF IMPERFECT FUNCTIONALLY GRADED CYLINDRICAL SHELLS

Babak Mirzavand and M. Reza Eslami

THERMOELASTIC STABILITY ANALYSIS OF IMPERFECT FUNCTIONALLY GRADED CYLINDRICAL SHELLS

BABAK MIRZAVAND AND M. REZA ESLAMI

Elastic buckling analysis of imperfect FGM cylindrical shells under axial compression in thermal environments is carried out, using two different models for geometrical imperfections. The material properties of the functionally graded shell are assumed to vary continuously through the thickness of the shell according to a power law distribution of the volume fraction of the constituent materials, also temperature dependency of the material properties is considered. Derivation of equations is based on classical shell theory using the Sanders nonlinear kinematic relations. The stability and compatibility equations for the imperfect FGM cylindrical shell are obtained, and the buckling analysis of shell is carried out using Galerkin's method. The novelty of the present work is to obtain closed form solutions for critical buckling loads of the imperfect FGM cylindrical shells, which may be easily used in engineering design applications. The effects of shell geometry, volume fraction exponent, magnitude of initial imperfections, and environment temperature on the buckling load are investigated. The results reveal that initial geometrical imperfections and temperature dependency of the material properties play major roles in dictating the bifurcation point of the functionally graded cylindrical shells under the action of axial compressive loads. Also results show that for a particular value of environment temperature, critical buckling load is almost independent of volume fraction exponent.

1. Introduction

An early attempt to establish occasional discrepancies between the theoretical and experimental buckling loads of cylindrical shells was reported in [Donnell 1934]. Later it was determined that the initial imperfections and the boundary conditions are the principal cause of disagreement. A well known buckling analysis of initially imperfect cylindrical shells is presented in [Donnell and Wan 1950; Donnell 1956]. The analysis is based on the equilibrium path of an imperfect cylindrical shell. Donnell's theory was later extended and applied to buckling problems by other researchers.

Recent studies on new performance materials have addressed new materials known as the functionally graded materials (FGMs). These are high-performance heat resistant materials able to withstand ultra high temperatures and minimize thermal stresses. The stabilization of a functionally graded cylindrical shell under axial harmonic loading is investigated in [Ng et al. 2001]. Shen [2002; 2003] (see also [Shen and Noda 2005]) presented the mechanical postbuckling of FGM cylindrical shells with temperature dependent properties in thermal environments under compressive axial loads and external pressure using a singular perturbation technique. The results reveal that the characteristics of postbuckling are significantly influenced by temperature rise and initial geometric imperfections. Shen [2004] also studied the thermal postbuckling of imperfect functionally graded cylindrical shells. Dynamic buckling of

functionally graded cylindrical thin shells under non-periodic impulsive loading is studied by [Sofiyev 2003]. [Shahsiah and Eslami 2003a; Shahsiah and Eslami 2003b] investigated the thermal buckling of functionally graded cylindrical shells under several types of loadings based on the Donnell and improved Donnell equations. [Woo et al. 2003; Woo et al. 2005] presented thermomechanical postbuckling analysis of functionally graded plates and shallow cylindrical shells based on the classical and higher order shell theories. [Mirzavand et al. 2005; Mirzavand and Eslami 2006] studied the thermal buckling of imperfect FGM cylindrical shells, under several types of loadings based on the Koiter and Wan–Donnell geometrical imperfection models. Also buckling and free vibration analysis of functionally graded cylindrical shells subjected to a temperature-specified boundary condition is investigated by [Kadoli and Ganesan 2006].

The present article develops the buckling analysis of imperfect functionally graded cylindrical shells under axial compression in thermal environments, using two different models for the geometrical imperfections; namely, the Koiter and Wan–Donnell Models. The cylindrical shell is graded according to a power law form through the thickness direction. The boundary conditions are assumed to be simply supported. The stability and compatibility equations for the imperfect FGM cylindrical shell are obtained, and the buckling analysis of the shell is carried out, using the Galerkin method, leading to the closed form solutions.

2. Fundamental equations

Consider a thin circular cylindrical shell of mean radius R and thickness h with length L made of functionally graded material. The shell is simply supported at its ends and subjected to a uniformly distributed axial compressive load P combined with thermal loading in the form of uniform temperature rise. The normal and shear strains at distance z from the shell middle surface are

$$\bar{\varepsilon}_x = \varepsilon_x + z\kappa_x, \qquad \bar{\varepsilon}_\theta = \varepsilon_\theta + z\kappa_\theta, \qquad \bar{\gamma}_{x\theta} = \gamma_{x\theta} + 2z\kappa_{x\theta}. \tag{1}$$

The middle-surface kinematic relations are

$$\varepsilon_x = u_{,x} + \tfrac{1}{2}\beta_x^2, \qquad \varepsilon_\theta = \frac{w + v_{,\theta}}{R} + \tfrac{1}{2}\beta_\theta^2, \qquad \gamma_{x\theta} = \frac{u_{,\theta}}{R} + v_{,x} + \beta_x\beta_\theta, \tag{2}$$

where u, v, w are the displacement components at points on the shell middle surface, and ε_x, ε_θ and $\gamma_{x\theta}$ are the middle surface normal and shear strains, respectively. The indices x and θ refer to the axial and circumferential directions, respectively. The rotations are

$$\beta_x = -w_{,x}, \qquad \beta_\theta = -\frac{w_{,\theta}}{R} \tag{3}$$

and the curvature components are

$$\kappa_x = \beta_{x,x}, \qquad \kappa_\theta = \frac{\beta_{\theta,\theta}}{R}, \qquad \kappa_{x\theta} = \frac{1}{2}\left(\frac{\beta_{x,\theta}}{R} + \beta_{\theta,x}\right). \tag{4}$$

The variation of Young's modulus and of the coefficient of thermal expansion of the functionally graded material are given by

$$E(z) = E_m + (E_c - E_m)\left(\frac{2z + h}{2h}\right)^\xi, \qquad \alpha(z) = \alpha_m + (\alpha_c - \alpha_m)\left(\frac{2z + h}{2h}\right)^\xi, \tag{5}$$

(see [Praveen and Reddy 1998]) where the subscripts m and c refer to the metal and ceramic constituents, and ξ is the volume fraction exponent which takes values greater than or equal to zero. The Poisson's ratio ν is considered to be constant across the thickness.

The force and moment resultants are [Mirzavand and Eslami 2006]

$$N_x = C(\varepsilon_x + \nu\varepsilon_\theta) + B(k_x + \nu k_\theta) - T_0, \qquad N_\theta = C(\varepsilon_\theta + \nu\varepsilon_x) + B(k_\theta + \nu k_x) - T_0,$$
$$M_x = B(\varepsilon_x + \nu\varepsilon_\theta) + D(k_x + \nu k_\theta) - T_1, \qquad M_\theta = B(\varepsilon_\theta + \nu\varepsilon_x) + D(k_\theta + \nu k_x) - T_1, \tag{6}$$

$$N_{x\theta} = \tfrac{1}{2}C(1-\nu)\gamma_{x\theta} + B(1-\nu)k_{x\theta},$$
$$M_{x\theta} = \tfrac{1}{2}B(1-\nu)\gamma_{x\theta} + D(1-\nu)k_{x\theta}, \tag{7}$$

where

$$C = \frac{h}{1-\nu^2}\left(E_m + \frac{E_{cm}}{\xi+1}\right), \quad B = \frac{h^2 E_{cm}}{2(1-\nu^2)}\left(\frac{\xi}{\xi^2+3\xi+2}\right), \quad D = \frac{h^3}{4(1-\nu^2)}\left(\frac{E_m}{3} + \frac{E_{cm}(\xi^2+\xi+2)}{\xi^3+6\xi^2+11\xi+6}\right),$$

$$T_0 = \frac{\Delta T h}{1-\nu}\left(E_m\alpha_m + \frac{E_m\alpha_{cm}+E_{cm}\alpha_m}{\xi+1} + \frac{E_{cm}\alpha_{cm}}{2\xi+1}\right), \qquad T_1 = \frac{1}{1-\nu}\int_{-h/2}^{+h/2} E\alpha\,\Delta T\,z\,dz. \tag{8}$$

Here ΔT is temperature rise from some reference temperature at which there are no thermal stresses.

The equilibrium equations of a perfect FGM cylindrical shell may be derived on the basis of the stationary potential energy criterion, and are given by [Mirzavand and Eslami 2006]

$$RN_{x,x} + N_{x\theta,\theta} = 0, \qquad N_{\theta,\theta} + RN_{x\theta,x} = 0,$$
$$\left(D - \frac{B^2}{C}\right)\nabla^4 w + \frac{1}{R}N_\theta - \left(N_x w_{,xx} + \frac{2}{R}N_{x\theta}w_{,x\theta} + \frac{1}{R^2}N_\theta w_{,\theta\theta}\right) = 0 \tag{9}$$

3. Analysis

Here the buckling analysis is presented for two common types of axisymmetric imperfections. According to the Koiter model, the axisymmetric geometrical imperfection of cylindrical shell is expressed as [Brush and Almroth 1975]

$$w^* = -\mu h\cos\left(\frac{m\pi x}{L}\right), \qquad -\frac{L}{2} \geq x \geq +\frac{L}{2}, \tag{10}$$

where m is the number of half wave in x-direction, and μh represents the amplitude of imperfection of the middle surface of the shell ($0 \leq \mu \leq 1$).

Donnell divides the initial imperfections into two combined components. Based on the experience with buckling problems, only that component which has the same shape as the deflection of the shell under load, which is w, can be taken into consideration [Donnell and Wan 1950; Donnell 1956]. Accordingly, the Wan–Donnell model for the axisymmetric radial imperfection is

$$w^* = \left(\frac{k-1}{2}\right)w, \tag{11}$$

where the coefficient k is the imperfection parameter, which is a constant number equal or greater than 1. The magnitude of k depends on the material properties and manufacturing process of the cylindrical shell. The value of $k = 1$ represents a perfect shell.

The unloaded shell in the imperfection form, including w^*, is assumed to be stress free. The small angle of rotation $w_{,x}$ in the equations for an initially perfect cylinder is replaced by $(w + w^*)_{,x}$. The form of the equations can be simplified substantially by introducing a circumferential coordinate $y = R\theta$. Using Equations (2) and (3) and by introducing the coordinate y, the net strains for the imperfect cylindrical shell now become

$$\varepsilon_x = u_{,x} + \tfrac{1}{2}w_{,x}^2 + w_{,x}^* w_{,x}, \qquad \varepsilon_y = v_{,y} + \frac{w}{R} + \tfrac{1}{2}w_{,y}^2, \qquad \gamma_{xy} = u_{,y} + v_{,x} + (w + w^*)_{,x} w_{,y}. \quad (12)$$

Similarly, Equations (9) for an initially imperfect cylindrical shell are replaced by

$$N_{x,x} + N_{xy,y} = 0, \qquad N_{xy,x} + N_{y,y} = 0,$$

$$\left(D - \frac{B^2}{C}\right)\nabla^4 w + \frac{1}{R}N_y - \left(N_x(w + w^*)_{,xx} + 2N_{xy}w_{,xy} + N_y w_{,yy}\right) = 0. \quad (13)$$

The stability equations of FGM cylindrical shell may be obtained by the application of the minimum potential energy criterion, and are [Mirzavand and Eslami 2006]

$$N_{x1,x} + N_{xy1,y} = 0, \qquad N_{xy1,x} + N_{y1,y} = 0,$$

$$\left(D - \frac{B^2}{C}\right)\nabla^4 w_1 + \frac{N_{y1}}{R}$$

$$-\left(N_{x1}(w_0 + w^*)_{,xx} + 2N_{xy1}w_{0,xy} + N_{y1}w_{0,yy} + N_{x0}w_{1,xx} + N_{y0}w_{1,yy} + 2N_{xy0}w_{1,xy}\right) = 0, \quad (14)$$

where u_0, v_0, w_0 are related to the equilibrium configuration, and u_1, v_1, w_1 are arbitrary small neighboring increments, and N_{ij1} represent the force resultants related to the neighboring state. Introducing the Airy stress function Φ as

$$N_{x1} = \Phi_{,yy}, \qquad N_{y1} = \Phi_{,xx}, \qquad N_{xy1} = -\Phi_{,xy} \quad (15)$$

the first and second stability equations are automatically satisfied and the third stability equation reduces to

$$\left(D - \frac{B^2}{C}\right)\nabla^4 w_1 + \frac{\Phi_{,xx}}{R}$$

$$-\left(\Phi_{,yy}(w_0 + w^*)_{,xx} - 2\Phi_{,xy}w_{0,xy} + \Phi_{,xx}w_{0,yy} + N_{x0}w_{1,xx} + N_{y0}w_{1,yy} + 2N_{xy0}w_{1,xy}\right) = 0. \quad (16)$$

The compatibility equation in terms of the Airy stress function and the lateral displacement component w_1 is [Mirzavand and Eslami 2006]

$$\nabla^4 \Phi - C(1 - v^2)\left(\frac{w_{1,xx}}{R} - (w_0 + w^*)_{,xx}w_{1,yy} + 2w_{0,xy}w_{1,xy} - w_{1,xx}w_{0,y}\right) = 0. \quad (17)$$

3.1. *Koitr imperfection model.* Equations (16) and (17) are a set of linear equations in terms of the variable prebuckling coefficients N_{ij0}, w_0, and the radial geometric imperfection w^*. The prebuckling coefficients must be known to be able to obtain the buckling load. Consider an imperfect cylindrical shell made of functionally graded material with simply supported edge conditions and subjected to axial compression load P. For the axisymmetric configuration on the primary path, $u_0 = u_0(x)$, $v_0 \equiv 0$, $w_0 = w_0(x)$ [Brush and Almroth 1975]. For the axisymmetric loading, $N_{xy0} = 0$ and from the first equilibrium equation, however, N_{xx0} is seen to be independent of x. Considering the boundary conditions at the cylinder

ends, where the axial load P is uniformly distributed around the circumference, the axial prebuckling force resultant is

$$N_{x0} = -\frac{P}{2\pi R} - T_0 = -\sigma h - T_0. \tag{18}$$

Using Equation (18) and the equilibrium equations, the other prebuckling coefficients are found to be

$$N_{y0} = C(1 - v^2)\frac{w_0}{R} - v\sigma h - T_0, \tag{19}$$

$$w_0 = \frac{vR(\sigma h + T_0)}{C(1 - v^2)} + q\cos\frac{m\pi x}{L}, \tag{20}$$

where

$$q = -\mu h \frac{(\sigma h + T_0)\left(\frac{m\pi}{L}\right)^2}{\left(D - \frac{B^2}{C}\right)\left(\frac{m\pi}{L}\right)^4 - \sigma h\left(\frac{m\pi}{L}\right)^2 + \frac{C(1 - v^2)}{R^2}}. \tag{21}$$

Introducing the prebuckling coefficients from the above equations into (16) and (17), we obtain the coupled linear equations of stability and compatibility as

$$\left(D - \frac{B^2}{C}\right)\nabla^4 w_1 + \frac{\Phi_{,xx}}{R} + \left((\sigma h + T_0)w_{1,xx} - \frac{C(1 - v^2)q}{R}\cos\frac{m\pi x}{L}w_{1,yy}\right.$$
$$\left. - \Phi_{,yy}(\mu h - q)\left(\frac{m\pi}{L}\right)^2\cos\frac{m\pi x}{L}\right) = 0,$$

$$\nabla^4\Phi - C(1 - v^2)\left(\frac{w_{1,xx}}{R} - w_{1,yy}(\mu h - q)\left(\frac{m\pi}{L}\right)^2\cos\frac{m\pi x}{L}\right) = 0. \tag{22}$$

To solve this system of equations, with the consideration of the simply supported boundary conditions, the approximate solutions may be considered as

$$w_1 = \alpha_{mn}\cos\frac{m\pi x}{L}\cos\frac{ny}{R}, \qquad \Phi = \beta_{mn}\cos\frac{m\pi x}{L}\cos\frac{ny}{R},$$
$$+\frac{L}{2} \geq x \geq -\frac{L}{2}, \qquad 2\pi R \geq y \geq 0, \qquad m, n = 1, 2, \ldots, \tag{23}$$

where m and n are the number of half waves in x and y-directions, respectively, and α_{mn} and β_{mn} are constant coefficients that depend on m and n. Substituting the approximate solutions (23) into Equations (22) gives the residues R_1 and R_2. Following Galerkin's method, R_1 and R_2 are made orthogonal with respect to the approximate solutions (23), and then the determinant of the obtained system of equations for the coefficients α_{mn} and β_{mn} is set to zero. For even values of m the determinant of coefficients has no result, but for $m = 4k \pm 1$ (odd values of m) yields

$$s_1(\sigma h + T_0)^3 + s_2(\sigma h + T_0)^2 + s_3(\sigma h + T_0) + s_4 = 0, \tag{24}$$

where we have set

$$s_1 = -f_1 f_2, \qquad s_2 = f_3 f_4 f_5^2 + f_5(f_3 f_6 + f_4 f_7 - f_1 f_8) - 2f_1 f_2 f_9 + f_6 f_7 - f_1 f_{10},$$
$$s_3 = f_5 f_9(f_3 f_6 + f_4 f_7 - f_1 f_8) - f_1 f_2 f_9^2 + 2f_9(f_6 f_7 - f_1 f_{10}), \qquad s_4 = f_9^2(f_6 f_7 - f_1 f_{10}),$$

with

$$f_1 = \frac{\pi R L}{2}\left(\left(\frac{m\pi}{L}\right)^4 + 2\left(\frac{m\pi}{L}\right)^2\left(\frac{n}{R}\right)^2 + \left(\frac{n}{R}\right)^4\right),$$

$$f_2 = -\frac{\pi R L}{2}\left(\frac{m\pi}{L}\right)^2,$$

$$f_3 = \frac{\pm 4RLC(1-\nu^2)}{3m}\left(\frac{m\pi}{L}\right)^2\left(\frac{n}{R}\right)^2,$$

$$f_4 = \frac{\mp 4RL}{3m}\left(\frac{m\pi}{L}\right)^2\left(\frac{n}{R}\right)^2,$$

$$f_5 = \mu h,$$

$$f_6 = \frac{-\pi R L}{2R}\left(\frac{m\pi}{L}\right)^2 \pm \frac{4RL\mu h}{3m}\left(\frac{m\pi}{L}\right)^2\left(\frac{n}{R}\right)^2,$$

$$f_7 = \frac{\pi R L C(1-\nu^2)}{2R}\left(\frac{m\pi}{L}\right)^2 \mp \frac{4RL\mu h}{3m}C(1-\nu^2)\left(\frac{m\pi}{L}\right)^2\left(\frac{n}{R}\right)^2,$$

$$f_8 = \frac{\pm 4RLC(1-\nu^2)}{3mR}\left(\frac{n}{R}\right)^2,$$

$$f_9 = -\left(D - \frac{B^2}{C}\right)\left(\frac{m\pi}{L}\right)^2 - \frac{C(1-\nu^2)}{R^2}\left(\frac{m\pi}{L}\right)^{-2},$$

$$f_{10} = \frac{\pi R L}{2}\left(D - \frac{B^2}{C}\right)\left(\left(\frac{m\pi}{L}\right)^4 + 2\left(\frac{m\pi}{L}\right)^2\left(\frac{n}{R}\right)^2 + \left(\frac{n}{R}\right)^4\right).$$

Solving (24) yields $\sigma h + T_0$ versus the material properties, the shell geometry parameters, the imperfection amplitude, and m and n. The critical axial compression load, in which buckling occurs, can be written as

$$P_{\mathrm{cr}} = 2\pi R(\sigma h)_{\min},\tag{25}$$

where P_{cr} is the critical axial compression load, and $(\sigma h)_{\min}$ is obtained by minimizing the solutions of (24) with respect to m and n.

3.2. Wan–Donnell imperfection model. Similarly, for an FGM cylindrical shell with the Wan–Donnell imperfection model, the prebuckling force resultants and prebuckling deflection may be found to be

$$N_{x0} = -\frac{P}{2\pi R} - T_0 = -\sigma h - T_0, \qquad N_{y0} = C(1-\nu^2)\frac{w_0}{R} - \nu\sigma h - T_0, \qquad N_{xy0} = 0 \tag{26}$$

and

$$w_0 = \eta \sin\frac{m\pi x}{L},\tag{27}$$

where

$$\eta = \frac{4(\nu\sigma h + T_0)/m\pi R}{\left(D - \dfrac{B^2}{C}\right)\left(\dfrac{m\pi}{L}\right)^4 - (\sigma h + T_0)\left(\dfrac{k+1}{2}\right)\left(\dfrac{m\pi}{L}\right)^2 + \dfrac{C(1-\nu^2)}{R^2}}.\tag{28}$$

Introducing the prebuckling coefficients from the above equations into Equations (16) and (17), result in the coupled linear equations of stability and compatibility as

$$\left(D - \frac{B^2}{C}\right) w_{1,xxxx} + \frac{\Phi_{,xx}}{R} - \Phi_{,yy}\left(\frac{k+1}{2}\right)\left(\frac{m\pi}{L}\right)^2 \eta \sin\left(\frac{m\pi x}{L}\right) + (\sigma h + T_0) w_{1,xx} = 0,$$

$$\nabla^4 \Phi - C(1-v^2)\frac{w_{1,xx}}{R} = 0. \tag{29}$$

To solve the system (29), with the consideration of the simply supported boundary conditions, the approximate solutions may be considered as

$$w_1 = \alpha_m \sin\frac{m\pi x}{L}, \qquad \Phi = \beta_{mn} \sin\frac{m\pi x}{L} \cos\frac{ny}{R},$$

$$L \geq x \geq 0, \ 2\pi R \geq y \geq 0, \qquad m, n = 1, 2, \ldots, \tag{30}$$

where m and n are the number of half waves in x and y-directions, respectively, and α_m and β_{mn} are constant coefficients that depend on m and n. Substituting the approximate solutions (30) into (29) gives the residues R_1 and R_2. Following Galerkin's method, R_1 and R_2 are made orthogonal with respect to the approximate solutions given by (30), and then the determinant of the resulting system of equations for the coefficients α_m and β_{mn} is set to zero, which for the odd values of m yields

$$\eta = \frac{-\pi}{\left(\frac{n}{R}\right)^2 \left(\frac{k+1}{2}\right)\left(\frac{8R}{3m}\right)}. \tag{31}$$

Considering (28) and (31), we obtain

$$\frac{P}{2\pi R} = \frac{\frac{C\pi(1-v^2)}{R^2} + \pi\left(D - \frac{B^2}{C}\right)\left(\frac{m\pi}{L}\right)^4 - T_0\left(\frac{k+1}{2}\right)\left(-\left(\frac{n}{R}\right)^2\left(\frac{32}{3m^2\pi}\right) + \pi\left(\frac{m\pi}{L}\right)^2\right)}{\left(\frac{k+1}{2}\right)\left(-\left(\frac{n}{R}\right)^2\left(\frac{32v}{3m^2\pi}\right) + \pi\left(\frac{m\pi}{L}\right)^2\right)}. \tag{32}$$

The critical axial compression load P_{cr} is obtained by minimizing this with respect to m and n.

4. Numerical results and discussion

The functionally graded materials chosen are zirconium oxide, ZrO_2, and the titanium alloy Ti-6Al-4V. Their material properties P are given in [Touloukian 1967] as functions of temperature T, of the form

$$P = P_0\left(1 + P_1 T + P_2 T^2 + P_3 T^3\right) \tag{33}$$

in which $T = T_0 + \Delta T$ and $T_0 = 300\,\text{K}$ (room temperature), and P_0, P_1, P_2, and P_3 are temperature dependent coefficients that are unique to the constituent materials. Typical values for Young's modulus E, Poison's ratio v, and the coefficient of thermal expansion α of zirconium oxide and titanium alloy are listed in Table 1. (A term in T^{-1} in Touloukian's version of (33) has coefficient zero in this case and is omitted.)

Here three comparison cases are presented for the validation of the results. The first comparison is based on the buckling under axial compression in the absence of thermal loading. Let us assume $\mu = 0$ and $k = 1$, in the Koiter and Wan–Donnell models, respectively, which corresponds to the equations for

| | ZrO$_2$ | | | | Ti-6Al-4V | | | |
	P_0	P_1	P_2	P_3	P_0	P_1	P_2	P_3
E (Pa)	$244.27 \cdot 10^9$	$-1.371 \cdot 10^{-3}$	$1.214 \cdot 10^{-6}$	$-3.681 \cdot 10^{-10}$	$122.56 \cdot 10^9$	$-4.586 \cdot 10^{-4}$	0	0
α (Pa)	$12.766 \cdot 10^{-6}$	$-1.491 \cdot 10^{-3}$	$1.006 \cdot 10^{-5}$	$-6.778 \cdot 10^{-11}$	$7.5788 \cdot 10^{-6}$	$6.638 \cdot 10^{-4}$	$-3.147 \cdot 10^{-6}$	0
ν	0.28	0	0	0	0.28	0	0	0

Table 1. Temperature-dependent thermoelastic coefficients for zirconium oxide ZrO$_2$ and titanium alloy Ti-6Al-4V. From [Touloukian 1967].

thickness ratio, h/R	0.003	0.004	0.005	0.006
this article (Koiter model)	2.40	4.26	6.65	9.58
this article (Wan–Donnell model)	2.52	4.26	6.77	9.66
[Brush and Almroth 1975]	2.40	4.26	6.65	9.58

Table 2. Buckling loads P_{cr} (in MN) for perfect homogeneous shells, in the absence of thermal load ($E = 70$ GPa, $\alpha = 23 \times 10^{-6}$/K, $\nu = 0.3$, $L/R = 1$).

volume fraction exponent ξ	0.0	0.2	0.5	1.0	2.0	3.0	5.0
this article (Koiter model)	85.90	95.65	106.49	118.74	133.12	141.62	151.59
this article (Wan–Donnell model)	87.89	97.68	108.91	121.81	137.05	145.98	156.27
[Shen 2004]	86.65	96.03	106.54	118.45	132.44	140.69	150.28

Table 3. Buckling temperature difference ΔT_{cr} for perfect FGM cylindrical shells, in the absence of axial compression ($h/r = 0.025$, $L/R = 0.866$).

a perfect cylindrical shell. If, in addition, we take $E_c = E_m$ and $\alpha_c = \alpha_m$ (pure homogeneous metallic shell), the solutions may be validated with the closed form solution obtained in [Brush and Almroth 1975] when $\Delta T = 0$. Table 2 shows the results obtained for a cylindrical shell made of pure aluminum ($L/R = 1$) with the Koiter and Wan–Donnell imperfection models discussed in this article, together with the values given by the closed form solution of Brush and Almorth. The comparison for the two imperfection models, when imperfections are eliminated, is well justified.

Other comparisons are based on the buckling under thermal loading in the absence of axial compression. Assume $\mu = 0$ and $k = 1$, in the Koiter and Wan–Donnell models, respectively (perfect cylindrical shell). For uniform temperature rise loading, in the absence of axial compression, the solution may be validated with the results obtained in [Shen 2004] for FGM shells made from Si$_3$N$_4$/SUS304 as shown in Table 3. If, in addition, we take $E_c = E_m$ and $\alpha_c = \alpha_m$ (homogenous shell), the solution may be validated with the closed form solution obtained in [Eslami et al. 1996] for an isotropic cylindrical shell, as shown in Table 4. As seen, in all cases the comparisons are well justified.

Figure 1 plots the variation of the ratio of critical load for the imperfect FGM cylindrical shell P_{cr} to the critical load of the corresponding perfect shell P_{ps}, subjected to axial compression and under

	Si$_3$N$_4$			SUS 304		
h/r	0.003	0.005	0.010	0.003	0.005	0.010
this article (Koiter model)	216.42	361.01	721.29	103.07	171.84	343.52
this article (Wan–Donnell model)	216.55	360.84	721.55	103.14	171.86	343.64
[Eslami et al. 1996]	216.61	360.79	722.03	103.16	171.94	343.87

Table 4. Buckling temperature difference ΔT_{cr} for perfect homogenous cylindrical shells, in the absence of axial compression. ($L/R = 0.866$)
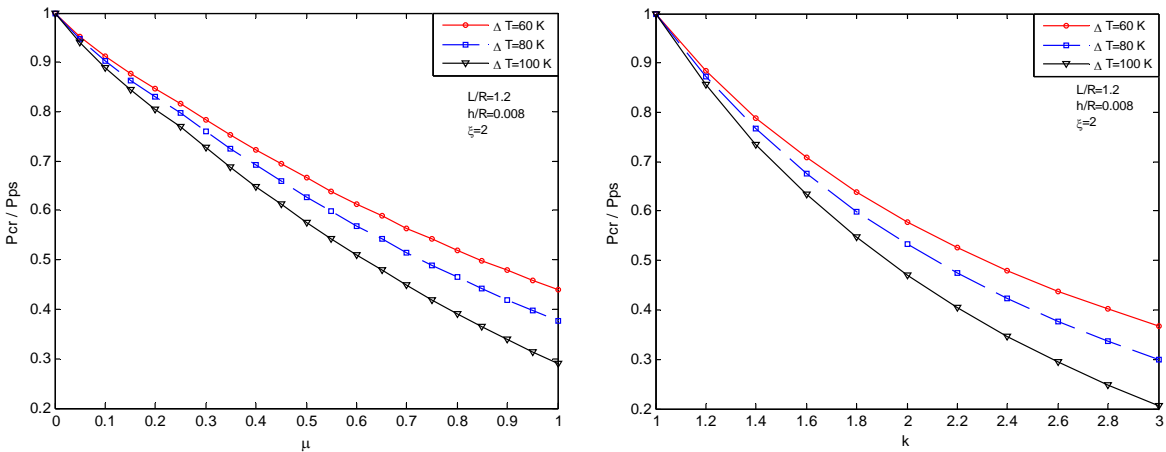
Figure 1. Influence of imperfection magnitude. Left: Koiter imperfection model; right Wan–Donnell imperfection model.

different uniform temperature rise and based on the Koiter imperfection parameter μ and Wan–Donnell imperfection parameter k for $L/R = 1.2$, $h/R = 0.008$, and $\xi = 2$. As the magnitude of imperfection increases, the buckling ratio decreases. This effect is stronger as the uniform temperature rise increases.

The influence of cylindrical shell geometry on critical axial compression load P_{cr} under a uniform temperature rise $\Delta T = 30\,\text{K}$ for various values of the volume fraction exponent $\xi = 0.5$, 1, 2 (as well as pure metal and pure ceramic) are illustrated in Figures 2 and 3. Figure 2 shows the buckling loads versus h/R for two imperfection models when the Koiter imperfection amplitude and Wan–Donnell imperfection parameter are 0.5 and 1.2, respectively, and $L/R = 1$. As the ratio h/R increases, the buckling load increases. Figure 3 represents the variation of buckling load versus L/R for two imperfection models when the Wan–Donnell imperfection parameter and the Koiter imperfection amplitude are 2 and 0.5, respectively, and $h/R = 0.005$. The critical bucking load increases as the ratio L/R increases.

The variation of P_{cr} versus volume fraction exponent are plotted for different values of environment temperature in Figure 4 for the two imperfection models. Here, the Koiter imperfection amplitude and Wan–Donnell imperfection parameter are 0.5 and 1.2, respectively, $L/R = 1.2$, and $h/R = 0.008$. As seen in this figures, for a particular value of environment temperature (here, $T = 350\,\text{K}$ for the Koiter model and $T = 360\,\text{K}$ for the Donnell model) the critical buckling load is almost constant for different
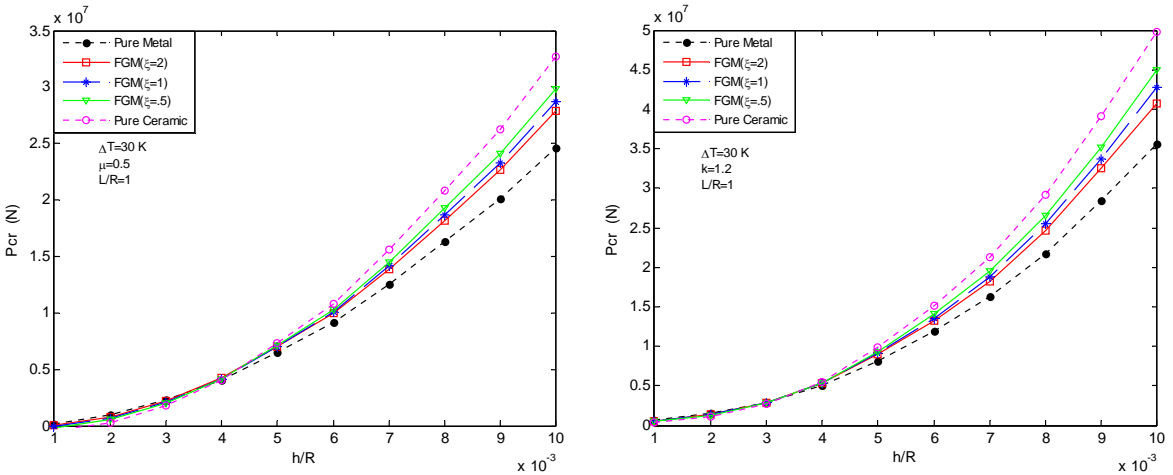
Figure 2. Variation of critical buckling load with h/R according to volume fraction exponent. Left: Koiter imperfection model; right Wan–Donnell imperfection model.
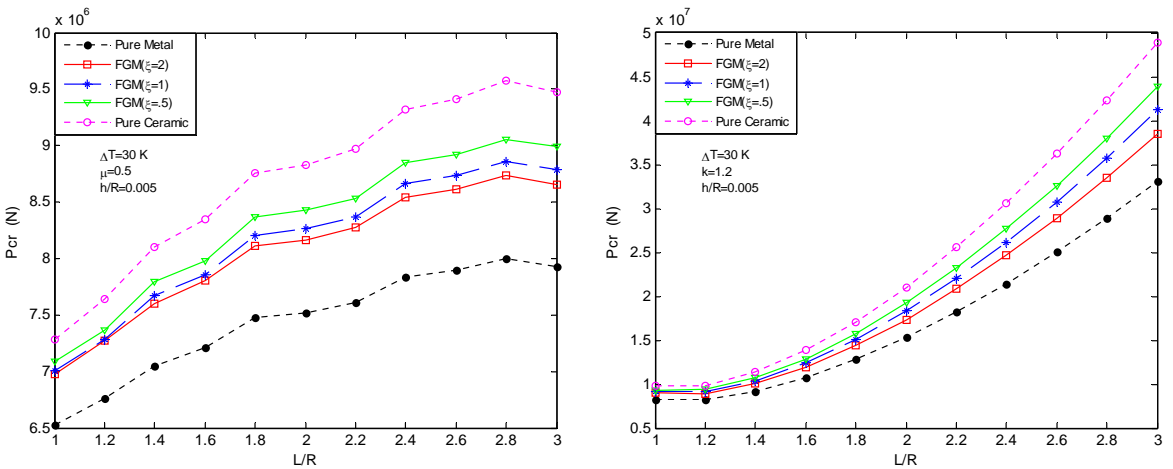

Figure 3. Variation of buckling load with L/R according to volume fraction exponent. Left: Koiter imperfection model; right Wan–Donnell imperfection model.

values of ξ, provided that the other parameters are kept constant. For temperatures less than this particular temperature, critical buckling load decreases as the volume fraction exponent ξ increases, and for temperatures greater than this particular temperature, critical buckling load increases as the volume fraction exponent ξ increases. This particular temperature, extremely depends on the shell parameters such as material properties, geometrical parameters, and magnitude of the initial imperfection. Note that negative values of P_{cr} in Figure 4, left for $T = 420\,\mathrm{K}(\Delta T = 120\,\mathrm{K})$ display situations that FGM cylindrical shell will buckle before applying any axial compression load, through existing thermal load (thermal buckling).
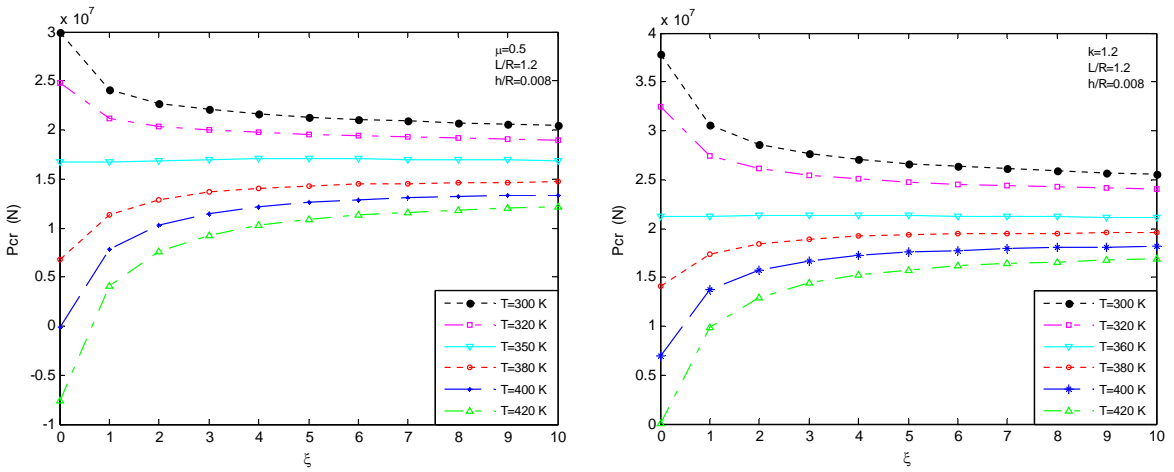
Figure 4. Critical buckling load of shell versus volume fraction exponent ξ and temperature T. Left: Koiter imperfection model; right Wan–Donnell imperfection model.

5. Conclusion

The equilibrium, stability, and compatibility equations for a simply supported imperfect functionally graded cylindrical shell are derived. The buckling analysis of imperfect FGM cylindrical shell under axial compressive load in thermal environments is investigated for two models of initial geometric imperfections, leading to the closed form solutions for the buckling load. The results reveal that effect of initial imperfections on decreasing the buckling load is stronger for larger magnitudes of the thermal loading. It is also shown that the buckling load of an imperfect functionally graded cylindrical shell subjected to thermomechanical loads increases with increasing the shell thickness and/or increasing shell length. Also results show that for a particular value of environment temperature, critical buckling load is almost independent of volume fraction exponent. Beyond this temperature, critical buckling load increases with increasing the volume fraction exponent and below that, critical buckling load decreases with increasing the volume fraction exponent.

References

[Brush and Almroth 1975] D. O. Brush and B. O. Almroth, *Buckling of bars, plates, and shells*, McGraw-Hill, New York, 1975.

[Donnell 1934] L. H. Donnell, "A new theory for the buckling of thin cylinders under axial compression and bending", *J. Appl. Mech.* (*ASME*) **56** (1934), 795–806.

[Donnell 1956] L. H. Donnell, "Effect of imperfections on buckling of thin cylinders under external pressure", *J. Appl. Mech.* (*ASME*) **23** (1956), 569–575.

[Donnell and Wan 1950] L. H. Donnell and C. C. Wan, "Effect of imperfections on buckling of thin cylinders and columns under axial compression", *J. Appl. Mech.* (*ASME*) **17** (1950), 73–83.

[Eslami et al. 1996] M. R. Eslami, A. R. Ziaii, and A. Ghorbanpour, "Thermoelastic buckling of thin cylindrical shells based on improved stability equations", *J. Therm. Stresses* **19**:4 (1996), 299–315.

[Kadoli and Ganesan 2006] R. Kadoli and N. Ganesan, "Buckling and free vibration analysis of functionally graded cylindrical shells subjected to a temperature-specified boundary condition", *J. Sound Vib.* **289**:3 (2006), 450–480.

[Mirzavand and Eslami 2006] B. Mirzavand and M. R. Eslami, "Thermal buckling of imperfect functionally graded cylindrical shells based on the Wan–Donnell model", *J. Therm. Stresses* **29**:1 (2006), 37–55.

[Mirzavand et al. 2005] B. Mirzavand, M. R. Eslami, and R. Shahsiah, "Effect of imperfections on thermal buckling of functionally graded cylindrical shells", *AIAA J.* **43**:9 (2005), 2073–2076.

[Ng et al. 2001] T. Y. Ng, Y. K. Lam, K. M. Liew, and J. N. Reddy, "Dynamic stability analysis of functionally graded cylindrical shells under periodic axial loading", *Int. J. Solids Struct.* **38**:8 (2001), 1295–1309.

[Praveen and Reddy 1998] G. N. Praveen and J. N. Reddy, "Nonlinear transient thermoelastic analysis of functionally graded ceramic-metal plates", *Int. J. Solids Struct.* **35**:33 (1998), 4457–4476.

[Shahsiah and Eslami 2003a] R. Shahsiah and M. R. Eslami, "Functionally graded cylindrical shell thermal instability based on improved Donnell equations", *AIAA J.* **41**:9 (2003), 1819–1826.

[Shahsiah and Eslami 2003b] R. Shahsiah and M. R. Eslami, "Thermal buckling of functionally graded cylindrical shell", *J. Therm. Stresses* **26**:3 (2003), 277–294.

[Shen 2002] H.-S. Shen, "Postbuckling analysis of axially-loaded functionally graded cylindrical shells in thermal environments", *Compos. Sci. Technol.* **62**:7–8 (2002), 977–987.

[Shen 2003] H.-S. Shen, "Postbuckling analysis of pressure-loaded functionally graded cylindrical shells in thermal environments", *Eng. Struct.* **25**:4 (2003), 487–497.

[Shen 2004] H.-S. Shen, "Thermal postbuckling behavior of functionally graded cylindrical shells with temperature-dependent properties", *Int. J. Solids Struct.* **41**:7 (2004), 1961–1974.

[Shen and Noda 2005] H.-S. Shen and N. Noda, "Postbuckling of FGM cylindrical shells under combined axial and radial mechanical loads in thermal environments", *Int. J. Solids Struct.* **42**:16–17 (2005), 4641–4662.

[Sofiyev 2003] A. H. Sofiyev, "Dynamic buckling of functionally graded cylindrical thin shells under non-periodic impulsive loading", *Acta Mech.* **165**:3–4 (2003), 151–163.

[Touloukian 1967] Y. S. Touloukian, *Thermophysical properties of high temperature solid materials*, MacMillan, New York, 1967.

[Woo et al. 2003] J. Woo, S. A. Meguid, and K. M. Liew, "Thermomechanical postbuckling analysis of functionally graded plates and shallow cylindrical shells", *Acta Mech.* **165**:1–2 (2003), 99–115.

[Woo et al. 2005] J. Woo, S. A. Meguid, J. C. Stranart, and K. M. Liew, "Thermomechanical postbuckling analysis of moderately thick functionally graded plates and shallow shells", *Int. J. Mech. Sci.* **47**:8 (2005), 1147–1171.

BABAK MIRZAVAND: bmirzavand@aut.ac.ir
Mechanical Engineering Department, Amirkabir University of Technology, Tehran 15914, Iran

M. REZA ESLAMI: eslami@aut.ac.ir
Mechanical Engineering Department, Amirkabir University of Technology, Tehran 15914, Iran
http://me.aut.ac.ir/M.Eslami.htm